THE JOURNAL OF PHYSICAL CHEMISTRY B

Article

pubs.acs.org/JPCB

Conformational Properties of Oxazole-Amino Acids: Effect of the Intramolecular N−H···N Hydrogen Bond

Dawid Siodłak,*[,†] Monika Staś,[†] Małgorzata A. Broda,[†] Maciej Bujak,[†] and Tadeusz Lis[‡]

[†]Faculty of Chemistry, University of Opole, Oleska 48, 45-052 Opole, Poland

[‡]Faculty of Chemistry, University of Wrocław, F. Joliot-Curie 14, 50-383 Wrocław, Poland

Supporting Information

ABSTRACT: Oxazole ring occurs in numerous natural peptides, but conformational properties of the amino acid residue containing the oxazole ring in place of the C-terminal amide bond are poorly recognized. A series of model compounds constituted by the oxazole-amino acids occurring in nature, that is, oxazole-alanine (L-Ala-Ozl), oxazole-dehydroalanine (ΔAla-Ozl), and oxazole-dehydrobutyrine ((*Z*)-ΔAbu-Ozl), was investigated using theoretical calculations supported by FTIR and NMR spectra and single-crystal X-ray diffraction. It was found that the main feature of the studied oxazole-amino acids is the stable conformation $\beta 2$ with the torsion angles φ and ψ of −150°, −10° for L-Ala-Ozl, −180°, 0° for ΔAla-Ozl, and −120°, 0° for (*Z*)-ΔAbu-Ozl, respectively. The conformation $\beta 2$ is stabilized by the intramolecular N−H···N hydrogen bond and predominates in the low polar environment. In the case of the oxazole-dehydroamino acids, the π-electron conjugation that is spread on the oxazole ring and $C^{\alpha}=C^{\beta}$ double bond is an additional stabilizing interaction. The tendency to adopt the conformation $\beta 2$ clearly decreases with increasing the polarity of environment, but still the oxazole-dehydroamino acids are considered to be more rigid and resistant to conformational changes.

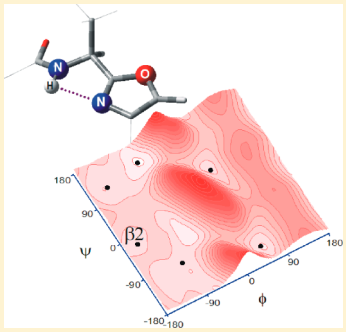

INTRODUCTION

Oxazole-amino acids (Xaa-Ozl) can be defined as amino acids with oxazole ring in place of the C-terminal amide group (Figure 1).

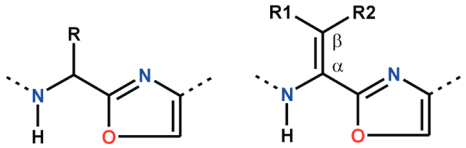

Figure 1. Schematic representation of oxazole-amino acid and oxazole-*α,β*-dehydroamino acid residues.

The oxazole-amino acids are present in numerous naturally occurring peptides,[1−22] which are produced by bacteria and which reveal potential antibiotics and antitumor activity.[23,24] In nature, the oxazole ring is formed by the cyclization of serine or threonine residues onto preceding amide carbonyl.[25] The oxazole-amino acids have also been used to modify peptides bioactivity,[26−28] and various synthetic procedures have been reported.[29−33] However, little is known about the influence of oxazole ring on the spatial arrangements of the natural as well as designed peptides.[34,35] In most cases, the natural oxazole-peptides are cyclic and contain many other structural modifications, so it is difficult to unambiguously determine the influence of the oxazole ring on peptides conformations. Among the natural oxazole-amino acids, alanine, valine, and glycine derivatives (Ala-Ozl, Val-Ozl, Gly-Ozl) have been found. There are also *α,β*-dehydroamino acids such as oxazole-dehydroalanine (ΔAla-Ozl) and oxazole (*Z*)-dehydrobutyrine ((*Z*)-ΔAbu-Ozl), which result from dehydratation of serine and threonine, respectively. The *α,β*-dehydroamino acids, due to the presence of the $C^{\alpha}=C^{\beta}$ double bond, and thus achiral *α*-carbon atom with sp^2 hybridization, reveal considerable influence on the conformation as well as the bioactivity of peptides. Dehydrophenylalanine is the most extensively studied *α,β*-dehydroamino acid residue.[36−42] In our previous studies we have shown that structural modifications of amino acids, such as methylation of the N-terminal amide bond[43,44] or introduction of the C-terminal ester group,[45−48] change the conformational preferences as compared with standard analogues. The aim of this work is a preliminary assessment of the influence of the oxazole ring in place of the C-terminal amide group on the conformational preferences of the amino acids. The studied structural motif can be useful in peptide design as well as in understanding the bioactive conformation of natural compounds containing the oxazole-amino acids as well as other closely related structures.[26,41,49] For this purpose a series of the model compounds **1**−**6** (Figure 2) containing oxazole amino acid residues were investigated using theoretical calculation (**1**−**3**) as well as spectroscopic NMR, IR, and single-crystal X-ray diffraction methods (**4**−**6**).

Received: December 12, 2013
Revised: February 12, 2014
Published: February 14, 2014

   dx.doi.org/10.1021/jp4121673 | *J. Phys. Chem. B* 2014, 118, 2340−2350

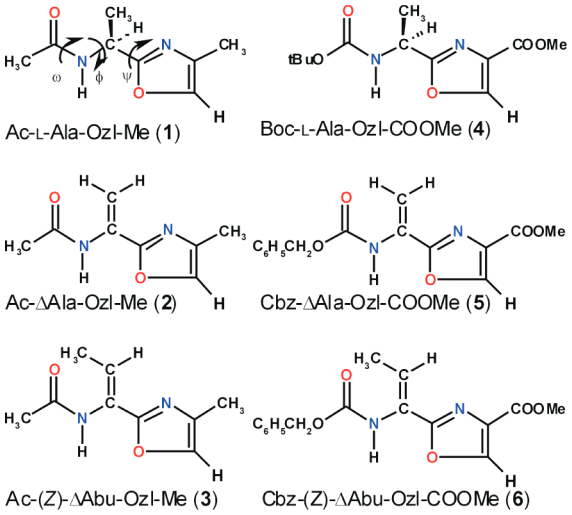

Figure 2. General formula and selected torsion angles for the model compounds studied in this work.

MATERIALS AND METHODS

Computational Procedures. The theoretical conformational properties of Ac-L-Ala-Ozl-Me (**1**), Ac-(*Z*)-ΔAbu-Ozl-Me (**2**), and Ac-ΔAla-Ozl-Me (**3**) were calculated using the Gaussian09 package.[50] Calculations were performed on molecules with the trans secondary amide groups ($\omega_0 \approx 180°$). The (φ, ψ) potential energy surfaces of the studied molecules were calculated at the meta-hybrid M06-2X/6-311++G(d,p)[51] levels of theory with resolutions of 30° for the main-chain (φ and ψ) dihedral angles. In each of the obtained structures, the geometrical parameters were fully relaxed, except for the constrained torsion angles φ and ψ. In the case of **2** and **3**, only half of the maps was computed because $E(\varphi,\psi) = E(-\varphi,-\psi)$. The energy surfaces were created using the Surfer 8 program.[52] To estimate the solvation effects on the shape of the Ramachandran maps, single-point calculations were also conducted in each grid point using a self-consistent reaction field (SCRF) model. Specifically, the SMD method has been chosen[53] following its successful application to the 4-metoxyproline diamide model.[54] Possible energy minima on the potential energy surfaces were investigated on every low-energy region of the map by full geometry optimization at the M06-2X, B3LYP, and MP2 levels in vacuo maintaining the same 6-311++G(d,p) basis set. To investigate the effect of environment of various polarity, we mimicked the presence of chloroform and water. The energy minima on the maps were fully optimized at the M06-2X/6-311++G(d,p) using the SMD model as well as at the B3LYP/6-311++G(d,p) and MP2/6-311++G(d,p) using the PCM model[55,56] previously applied for dehydroamino acids.[57] Frequency analyses were carried out to verify the nature of the minimum state of all stationary points obtained and to calculate the zero-point vibrational energies (ZPVEs).

Synthesis. *N-tert*-Butoxycarbonyl-L-alanine (Boc-Ala) was applied as purchased (Fluka). *N*-Benzyloxycarbonyldehydroalanine (*Z*-ΔAla) and *N*-benzyloxycarbonyl-(*Z*)-dehydrobutyrine (Cbz-(*Z*)-ΔAbu) were obtained by condensation of benzyl carbamate with pyruvic acid and 2-oxobutyric acid, respectively.[58,59] The corresponding dipeptides Boc-Ala-Ser-OMe, Cbz-ΔAla-Ser-OMe, and Cbz-(*Z*)-ΔAbu-Ser-OMe were obtained by coupling with serine methyl ester hydrochloride using *N,N′*-dicyclohexylcarbodiimide according to Bilcer et al.[60] The studied oxazole compounds were synthesized on the basis of the procedure described by Phillips et al.[29]

General Procedure. Glass round flask (10 mL), magnetic stirring, and cooling bath (mixture of acetone and liquid nitrogen) were used. Dipeptide, 1 mmol, (Boc-Ala-Ser-OMe or Cbz-(*Z*)-ΔAla-Ser-OMe or Cbz-(*Z*)-ΔAbu-Ser-OMe) was dissolved in dichloromethane, 10 mL, and then cooled to −70 °C. (Diethylamino)sulfur trifluoride (DAST), 1.1 mmol, was added dropwise to the reaction solution. At continuous stirring, for 60 min, temperature increased to −40 °C. 1,8-Diazabicyclo[5.4.0]undec-7-ene (DBU), 3.6 mmol, was added dropwise, and the yellow solution appeared. When temperature reached 0 °C (in ca. 60 min), $CBrCl_3$, 3.6 mmol, was added, and the dark brown solution appeared. The reaction mixture was stirred overnight at room temperature. The reaction was quenched with 5 mL of saturated aqueous sodium bicarbonate. Saturated sodium chloride solution, 5 mL, was added for a better phase separation; then, the mixture was extracted with ethyl acetate. The combined organic layer was dried (using anhydrous $MgSO_4$), filtered, and concentrated. The dark-brown concentrate was filtered on a Schott funnel through a 2 cm thick layer of silica gel (Kiesegel 60, Merck) and washed with ethyl acetate. The yellow filtrate was concentrated; then, the crude product was purified by flash chromatography (SiO_2—Kiesegel 60, hexane/ethyl acetate 2:1). The progress of purification was monitored by TLC with fluorescent indicator as well as potassium permanganate solution for the dehydroamino acid compounds **5** and **6** and chlorine/*o*-toluidine for the alanine compound **4**. The additional purification by flash chromatography (SiO_2, chloroform/acetone 90:10) might be required. Crystallization from diethyl ether/hexane solution at 5 °C gave white solid. Average yield: 40%. Methyl (*S*)-2-[1-(((*tert*-Butoxy)carbonyl)amino)et-1-yl]-1,3-oxazole-4-carboxylate (Boc-L-Ala-Ozl-COOMe) (**4**): white solid; mp 106.2 °C (DSC). ^{1}H NMR (400 MHz, DMSO-d_6) δ 8.80 (1H, s, Ozl ring-H), 7.60 (1H, d, J = 8.0 Hz, N*H*), 4.82 (1H, q, J = 7.2 Hz, C$^{\alpha}$-*H*), 3.80 (3H, s, O-C*H*$_3$), 1.42 (3H, d, J = 7.2 Hz, C$^{\beta}$-*H*), 1.26 (9H, s, *t*-Bu). ^{13}C NMR (400 MHz, DMSO-d_6) δ 165.34, 160.68, 154.44, 145.01, 131.54, 77.88, 51.28, 43.53, 27.67, 18.10. Anal. Calcd for $C_{12}H_{18}N_2O_5$ (270.29): C, 53.33; H, 6.71; N, 10.36. Found: C, 53.29; H, 6.55; N, 10.10%. Methyl 2-[1-((Benzyloxy)carbonyl)amino)et-1-en-1-yl]-1,3-oxazole-4-carboxylate (Cbz-ΔAla-Ozl-OMe) (**5**): white solid; mp 86.4 °C (DSC). ^{1}H NMR (400 MHz, DMSO-d_6) δ 9.36 (1H, s, N-*H*), 8.91 (1H, s, Ozl ring-H), 7.37 (5H, m, Ph ring-*H*), 5.67 (1H, s, C$^{\beta}$-(*Z*)-*H*), 5.63 (1H, s, C$^{\beta}$-(*E*)-*H*), 5.11 (2H, s, C*H*$_2$), 3.83 (3H, s, O−C*H*$_3$). ^{13}C NMR (400 MHz, DMSO-d_6) δ 160.39, 158.32, 153.31, 145.42, 135.84, 132.47, 129.02, 127.93, 127.54, 127,42, 117.60, 65.51, 51.44. Anal. Calcd for $C_{15}H_{14}N_2O_5$ (302.29): C, 59.60; H, 4.67; N, 9.27. Found: C, 59.38; H, 4.45; N, 9.11%. Methyl (*Z*)-2-[1-((Benzyloxy)carbonyl)amino)prop-1-en-1-yl]-1,3-oxazole-4-carboxylate (Cbz-(*Z*)-ΔAbu-Ozl-OMe) (**6**): white solid; mp 138.1 °C (DSC). ^{1}H NMR (400 MHz, DMSO-d_6) δ 9.13 (1H, s, N-*H*), 8.81 (1H, s, Ozl ring-H), 7.40 (5H, m, Ph ring-*H*), 6.47 (1H, q, J = 6.4 Hz, C$^{\beta}$-*H*), 5.09 (2H, s, C*H*$_2$), 3.81 (3H, s, O−C*H*$_3$), 1.78 (3H, d, J = 6.4 Hz, C$^{\gamma}$-*H*$_3$). ^{13}C NMR (400 MHz, DMSO-d_6) δ 160.61, 159.89, 153.73, 144.68, 136.11, 132.38, 127.91, 127.43, 127.40, 127,31, 123.35, 65.44, 51.36, 12.62. Anal. Calcd for $C_{16}H_{16}N_2O_5$ (316.32): C, 60.76; H, 5.10; N, 8.86. Found: C, 60.51; H, 4.98; N, 8.62%.

FTIR Spectroscopy. The IR spectra were recorded at room temperature using a Nicolet Nexus spectrometer equipped with

dx.doi.org/10.1021/jp4121673 | J. Phys. Chem. B 2014, 118, 2340−2350

DTGS detector and flushed with dry nitrogen during the measurements. The thickness of the KBr liquid cell was 2.86 mm. The concentration was between 8.6 and 12.8 × 10^{-3} mol/L. All spectra were recorded at the 1 cm^{-1} resolution and averaged using 100 scans. The solvent spectra obtained under the same conditions were subtracted from sample spectra. The spectra were analyzed using the GRAMS/A1 version 9 (Thermo Fisher Scientific). The number and position of component bands were obtained by Fourier self-deconvolution techniques and by means of the second derivative as an "initial guess". To determine the number of component bands, we also took the results of the quantum-mechanical calculations into account. Then, the accurate band positions were determined by the curve-fitting procedure with a mixed (Gauss−Lorentz) profile.

NMR Spectroscopy. The ^{1}H and ^{13}C NMR spectra were recorded in the $CDCl_3$ and DMSO-d_6 solutions, with internal TMS standard, on Bruker NMR Spectrometer Ultrashield 400 MHz (2005) at room temperature. Data acquisition and processing were performed using standard Bruker TopSpin version 1.3 software. The assignment of the conformations was achieved using the NOE difference method (mixing time 300 ms) within the standard programs. The NOE spectra were recorded using 12 000 scans for **4** and 4000 scans for **5** and **6**.

X-ray Crystal Structure Analysis. The single crystals of **4** and **6** were grown by slow evaporation of the diethyl ether/hexane solution at ca. 5 °C. The low-temperature X-ray diffraction intensity data for **4** (at 100(2) K) and for **6** (at 80(2) K) were collected on an Xcalibur diffractometer, with the graphite-monochromated MoKα radiation (λ = 0.71073 Å), equipped with a Ruby CCD detector and an Oxford Cryosystems cooler. The reflections were measured using the ω-scan technique. The data were subjected to Lorentz and polarization corrections. The CrysAlis CCD and CrysAlis RED programs were used during the data collection, cell refinement, and data reduction processes.[61] Both structures were solved by direct methods and refined on F^2 by the full-matrix least-squares method using SHELX-97.[62] All non-H atoms, in both structures, were refined with anisotropic displacement parameters. All of the H atoms were located in the subsequent difference Fourier maps and isotropically refined. The coordinates and displacement parameters of the H atoms attached to the N1 atom in the structure of **4** and **6** (and C32 atom in the case of **6**) were freely refined, whereas the refinement of the remaining H atoms was performed using a riding model. The displacement parameters of these H atoms, in both structures, were set at 1.5 and 1.2 times larger than the respective parameters of the methyl carbon and the remaining carbon atoms, respectively. The structure drawings were prepared using Mercury.[63]

The crystallographic data for **4** and **6** have been deposited at the Cambridge Crystallographic Data Centre as supplementary publication nos. CCDC 976532 and CCDC 976533, respectively. These data can be obtained free of charge via http://www.ccdc.cam.ac.uk/conts/retrieving.html or from the Cambridge Crystallographic Data Centre, 12 Union Road, Cambridge CB2 1EZ, U.K.; Fax: +44 1223 336 033; E-mail: deposit@ccdc.cam.ac.uk. Crystal Data for Boc-L-Ala-Ozl-COOMe (**4**). $C_{12}H_{18}N_2O_5$, M = 270.28, crystal size 0.46 × 0.23 × 0.02 mm, monoclinic, space group $P2_1$, a = 5.0917(12), b = 5.8080(13), c = 23.146(6) Å, β = 94.54(4)°, V = 682.3(3) $Å^3$, ρ_{calcd} = 1.316 g/cm^3, Z = 2, μ = 0.103 mm^{-1}, reflections collected 5796, R_{int} = 0.0249, data/parameters 3288/181, GOF on F^2 1.046, R_1 (all data) = 0.0627, wR_2 (all data) = 0.0956. Crystal Data for Cbz-(Z)-ΔAbu-Ozl-COOMe (**6**). $C_{16}H_{16}N_2O_5$, M = 316.31, crystal size 0.48 × 0.09 × 0.07 mm, monoclinic, space group $P2_1/n$, a = 4.7888(16), b = 51.115(17), c = 6.0277(18) Å, β = 94.59(4)°, V = 1470.7(8) $Å^3$, ρ_{calcd} = 1.429 g/cm^3, Z = 4, μ = 0.108 mm^{-1}, reflections collected 5088, R_{int} = 0.0238, data/parameters 3191/217, GOF on F^2 1.067, R_1 (all data) = 0.0526, wR_2 (all data) = 0.1010.

RESULTS

Theoretical Calculations. The conformational properties of the oxazole-alanine compound, Ac-L-Ala-Ozl-Me (**1**), are shown in Figure 3 and Table 1. In the gas phase, five different conformations are present: β2, C5, β, αD, and αL. The lowest in energy is the conformation β2 (φ, $\psi \approx -157°$, $-9°$) and then the conformation C5 (φ, $\psi \approx -153°$, $135°$). Both conformations are stabilized by intramolecular hydrogen bonds (N−H···N and N−H···O, respectively) formed between N−H group and a heteroatom of the oxazole ring. The conformation β (φ, $\psi \approx -50°$, $157°$) is also predicted but at the M06-2X and MP2 levels of theory. The conformations αD (φ, $\psi \approx 54°$, $-148°$) and αL (φ, $\psi \approx 55°$, $37°$) are the highest in energy order. In low polar chloroform environment, the preference toward the conformation β2 is retained. In contrast, the conformation C5 is energetically disfavored. Furthermore, the conformation α' appears, and its torsion angles φ and ψ vary in the range of −(123−144)° and −(84−117)° depending on the method used. The conformations αD and αL are still the highest in energy, although the differences are smaller. Increase in the environment polarity simulated by water favors the conformation β. The conformation β2 is predicted to be the lowest energy one only at the B3LYP level of theory. The energy differences between conformations are small and in almost all cases do not exceed 2 kcal/mol. The simulated changes of the environment seem to not influence the conformations β2 as well as αD. The differences in torsion angles do not exceed ±4°. The moderate changes, up to 13°, are observed for the conformation β and αL; however, the geometry of the conformations C5 and α' undergo changes up to 23 and 45°, respectively. The potential energy surface shows that these conformations are placed in the shallow regions, in which relatively small changes in energy result in considerable changes of the torsion angles.

Figure 4 presents the conformational properties of the oxazole-dehydroalanine model compound, Ac-ΔAla-Ozl-Me (**2**). Because of achirality of the molecule, the symmetry-related pairs of conformations with the same energy but opposite torsion angles are present. For clarity, only the conformations located at the left side of the map are analyzed. The four different conformations were found: β2, C5, β, and α ordered by the growth of energy in the gas phase, as predicted by all theoretical methods applied (Table 1). The most stable is the conformation β2 with the torsion angles φ, ψ of −180°, 0° for B3LYP and M06-2X and −168°, 6° for MP2 level of theory, respectively. The preference toward the conformation β2 seems to be independent of the simulated environment. Increase in the environment polarity decreases the energy difference between the conformations and, as is predicted by M06-2X and MP2 methods, favors the conformation β and disfavors the conformation C5, but the number and the type of conformations do not change. Also, the geometrical changes of the conformations do not exceed ±3°, except for the conformation C5 calculated at the MP2 level of theory. This

dx.doi.org/10.1021/jp4121673 | J. Phys. Chem. B 2014, 118, 2340−2350

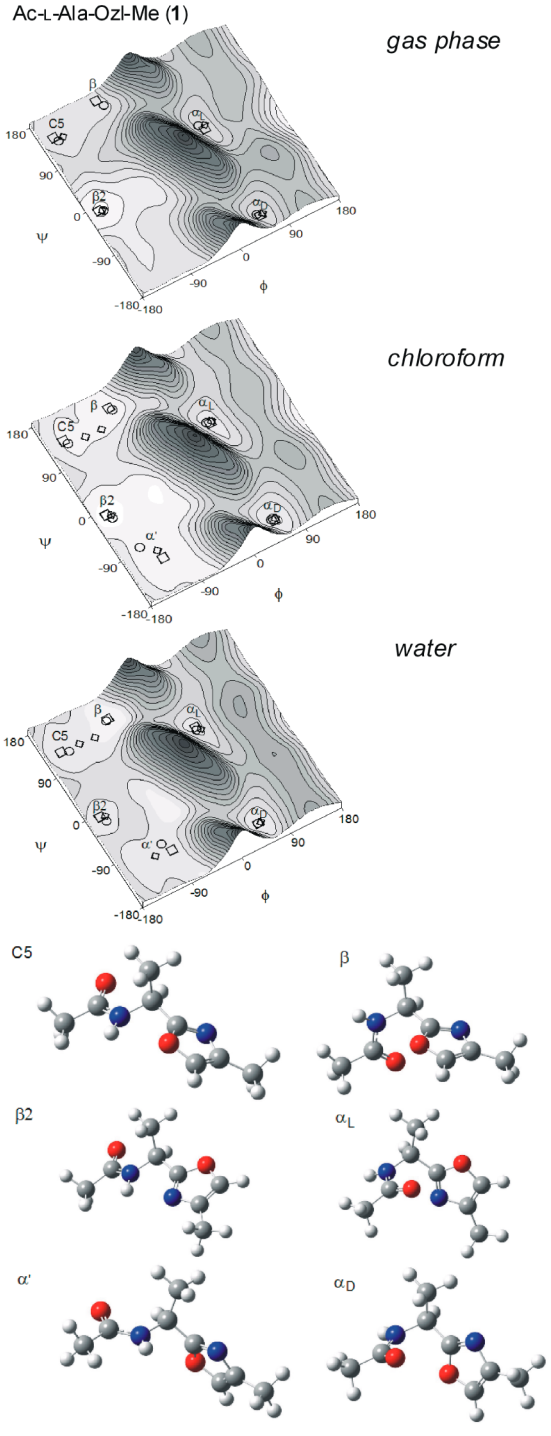

Figure 3. Potential energy surfaces $E = f(\varphi,\psi)$ for Ac-L-Ala-Ozl-Me (**1**) calculated by the M06-2X/6-311++G(d,p) method in gas phase, chloroform, and water. Energy contours are plotted every 1 kcal/mol. Local minima (see Table 1) are calculated at the M06-2X (□), B3LYP (◇), and MP2 (○) levels. The presented conformers were optimized at M06-2X/6-311++G(d,p) in chloroform.

shows a considerable conformational stability of the studied ΔAla-Ozl residue. The coplanarity of the oxazole ring, carbon−carbon double bond, and the N-terminal amide group in the conformations $\beta2$ and C5 should be noted.

Figure 5 depicts the conformational properties of the oxazole-(*Z*)-dehydrobutyrine, Ac-(*Z*)-ΔAbu-Ozl-Me (**3**). Similar to dehydroalanine analogue **2**, the conformation $\beta2$ ($\varphi, \psi \approx$ −124°, 2°) is the lowest in energy, regardless of the method applied and environment simulated (Table 1). All calculation methods provide the same number and type of conformations as for the model **2**, except for the conformation α, which is not predicted in the gas phase. The geometrical changes of the conformations do not exceed ±5°. Because of the presence of the methyl group in the side chain at the position *Z*, the torsion angle φ adopts the value of ca. −120° in the conformations $\beta2$ and C5 as compared with those in **2**. Also, the gap in energy between the conformations is smaller than in the case of the dehydroalanine analogue.

FTIR and NMR Spectroscopy. Figure 6 shows the ν_s(N−H)-stretching mode region of the Fourier transform infrared (FTIR) spectra of the studied compounds in nonpolar CCl_4 and weakly polar $CHCl_3$ solutions.

All bands observed in this region were assigned to the N−H-stretching vibrations of monomers. In the CCl_4 solution, the bands for the Ala-Ozl (**4**) and ΔAla-Ozl (**5**) residues have a symmetrical shape and are relatively narrow ($\Delta\nu_{1/2}$ = 29 and 19 cm^{-1}, respectively), which means that they originate from single conformations. The differences in width between these bands can be explained on the basis of the shape of the potential energy surface around the conformations (Figures 4 and 5). In the case of oxazole-dehydroalanine **5**, the potential energy minima are well-defined, and the geometry changes in the conformations are small. In contrast, the areas of the potential energy minima for saturated oxazole-alanine **4** are relatively broad, which result from the greater changes in geometry of the conformations taking place within the same range of energy. For (*Z*)-ΔAbu-Ozl (**6**), the band at 3409 cm^{-1} has a shoulder on the side of higher frequency, at 3436 cm^{-1}, which indicates a mixture of conformers. Deconvolution shows the main band, which comes from a conformer with strong H bond and a small amount of a conformer having weakly bonded N−H group. In $CHCl_3$ solution, all bands are wider, showing interactions with more polar solvent. Position of the ν_s(N−H) bands in CCl_4 solution at 3409−3442 cm^{-1} indicates the presence of an internal hydrogen bond involving the N−H group, weak for Ala-Ozl (**4**) and much stronger for oxazole-dehydroamino acids (**5** and **6**). On the basis of the theoretical analysis, two conformations can be considered: $\beta2$ with the N−H···N hydrogen bond, in which the nitrogen atom of the oxazole ring serves as a proton acceptor, and C5 with the N−H···O hydrogen bond, in which the oxazole oxygen atom is an acceptor. The calculated order of the stability of the conformation shows the lowest energy for the conformation $\beta2$. The theoretical frequencies of the acetyl analogues (**1**−**3**) shown in Table 1S in the Supporting Information, although somehow ambiguous depending on the method used, indicate that the bands at 3409 cm^{-1} for the ΔAla-Ozl and (*Z*)-ΔAbu-Ozl should be assigned to the conformation $\beta2$. Also, the band at 3442 cm^{-1} for Ala-Ozl should be assigned to the conformation $\beta2$. The band deconvolution for (*Z*)-ΔAbu-Ozl shows that the conformation C5 is also present.

Figure 7 presents the NOE difference experiment applied to study the conformational preferences in solution.

As can be seen in the conformations presented in Figures 3−5, the distance between selected hydrogen atoms depends on the adopted torsion angles. In particular, the distance between the hydrogen atom at the oxazole ring and hydrogen atom of the N-terminal N−H group as well as the hydrogen atom α in the case of Ala-Ozl together with the hydrogen atom β in the case of ΔAla-Ozl and (*Z*)-ΔAbu-Ozl can be useful to

dx.doi.org/10.1021/jp4121673 | J. Phys. Chem. B 2014, 118, 2340−2350

Table 1. Selected Torsion Angles (deg) and Thermodynamic Properties (kcal/mol) of Local Minima for Ac-L-Ala-Ozl-Me (1), Ac-(Z)-ΔAbu-Ozl-Me (2), and Ac-ΔAla-Ozl-Me (3)

Ac-L-Ala-Ozl-Me (1)											
B3LYP/6-311++G(d,p)				M06-2X/6-311++G(d,p)				MP2/6-311++G(d,p)			
conformer	φ	ψ	ΔE	conformer	φ	ψ	ΔE	conformer	φ	ψ	ΔE
	Gas Phase				Gas Phase				Gas Phase		
β2	−155.4	−9.5	0.00	β2	−160.5	−6.4	0.00	β2	−153.8	−10.1	0.00
C5	−144.6	134.2	1.83	C5	−158.8	140.3	2.41	C5	−154.6	131.6	1.76
αD	58.3	−148.1	4.31	β	−66.9	164.8	3.10	β	−60.1	150.9	1.90
αL	59.8	38.3	4.65	αD	53.6	−149.8	3.41	αL	50.0	41.7	2.56
				αL	56.3	31.5	3.56	αD	49.3	−145.4	2.65
	Chloroform				Chloroform				Chloroform		
β2	−152.3	−11.6	0.00	β2	−159.2	−8.3	0.00	β2	−153.5	−17.4	0.00
α′	−124.0	−101.7	0.66	β	−63.5	149.8	1.10	β	−60.3	144.4	0.33
C5	−120.0	122.0	0.92	α′	−122.6	−116.9	1.20	α′	−144.4	−84.1	0.60
β	−92.3	121.1	1.23	C5	−152.1	132.3	1.71	C5	−148.5	125.4	0.86
αD	57.3	−143.4	3.00	αD	53.7	−145.8	2.03	αD	50.7	−143.0	1.27
αL	57.3	49.2	3.57	αL	53.9	47.2	2.39	αL	49.2	50.1	1.66
	Water				Water				Water		
β2	−150.4	−11.3	0.00	β	−57.1	143.2	0.00	β	−60.5	141.1	0.00
α′	−118.2	−113.1	0.11	αD	51.9	−141.1	0.76	β2	−153.1	−20.2	0.76
β	−92.3	121.0	0.14	α′	−89.9	−115.8	1.13	α′	−99.1	−99.0	0.78
C5	−120.0	122.0	0.22	β2	−158.3	−8.7	1.14	αD	51.1	−141.0	0.89
αD	56.5	−141.2	1.88	αL	52.6	57.1	1.47	C5	−140.1	119.4	1.01
αL	57.5	49.1	2.65	C5	−152.2	124.5	1.47	αL	50.8	51.6	1.59
Ac-ΔAla-Ozl-Me (2)											
B3LYP/6-311++G(d,p)				M06-2X/6-311++G(d,p)				MP2/6-311++G(d,p)			
conformer	φ	ψ	ΔE	conformer	φ	ψ	ΔE	conformer	φ	ψ	ΔE
	Gas Phase				Gas Phase				Gas Phase		
β2	−180.0	0.0	0.00	β2	−180.0	0.0	0.00	β2	−168.0	5.7	0.00
C5	−180.0	180.0	2.84	C5	−179.9	−180.0	2.73	C5	−168.3	−166.5	3.11
β	−52.0	159.0	6.31	β	−50.6	159.0	6.62	β	−48.9	154.4	3.84
α	−57.8	−20.8	6.46	α	−57.8	−15.0	6.78	α	−50.1	−25.6	4.06
	Chloroform				Chloroform				Chloroform		
β2	−180.0	0.0	0.00	β2	−180.0	0.0	0.00	β2	−180.0	0.0	0.00
C5	−180.0	180.0	2.22	C5	−179.8	−179.9	2.03	β	−48.1	150.7	1.61
β	−52.5	156.8	4.33	β	−49.6	154.1	3.57	α	−52.9	−29.1	1.95
α	−60.2	−20.8	4.52	α	−56.8	−21.1	4.11	C5	−165.1	−163.2	2.02
	Water				Water				Water		
β2	−180.0	0.0	0.00	β2	−180.0	−0.1	0.00	β2	180.0	0.0	0.00
C5	−180.0	180.0	1.81	β	−47.0	147.9	0.58	β	−47.8	148.8	0.36
β	−52.7	155.0	3.16	C5	−179.8	−179.9	1.00	α	−54.0	−29.7	0.83
α	−62.1	−19.7	3.33	α	−58.8	−20.9	1.23	C5	−164.1	−160.8	1.46
Ac-(Z)-ΔAbu-Ozl-Me (3)											
B3LYP/6-311++G(d,p)				M06-2X/6-311++G(d,p)				MP2/6-311++G(d,p)			
conformer	φ	ψ	ΔE	conformer	φ	ψ	ΔE	conformer	φ	ψ	ΔE
	Gas Phase				Gas Phase				Gas Phase		
β2	−126.7	−1.8	0.00	β2	−126.1	−1.4	0.00	β2	−123.5	0.4	0.00
C5	−123.1	−175.4	1.93	C5	−124.6	−176.9	2.34	C5	−122.1	−168.1	2.27
β	−57.5	163.6	3.25	β	−52.8	161.9	4.95	β	−49.0	155.5	3.07
	Chloroform				Chloroform				Chloroform		
β2	−123.5	0.6	0.00	β2	−124.8	0.8	0.00	β2	−122.6	4.3	0.00
C5	−119.4	−172.4	1.18	C5	−122.7	−169.3	1.42	β	−49.7	152.6	1.25
β	−58.6	161.7	1.47	β	−52.2	157.5	2.05	α	−54.5	−25.2	1.39
α	−62.8	−14.7	1.95	α	−62.8	−14.7	2.50	C5	−121.3	−162.0	1.45
	Water				Water				Water		
β2	−120.8	3.1	0.00	β2	−122.0	6.9	0.00	β2	−121.6	8.5	0.00
α	−69.5	−12.3	0.43	β	−49.3	151.8	0.99	β	−49.7	150.7	0.18
β	−58.2	158.9	0.53	C5	−122.0	−164.6	1.19	α	−55.9	−26.5	0.49
C5	−117.0	−171.0	0.79	α	−60.8	−17.5	1.63	C5	−121.1	−159.1	1.00

dx.doi.org/10.1021/jp4121673 | J. Phys. Chem. B 2014, 118, 2340−2350

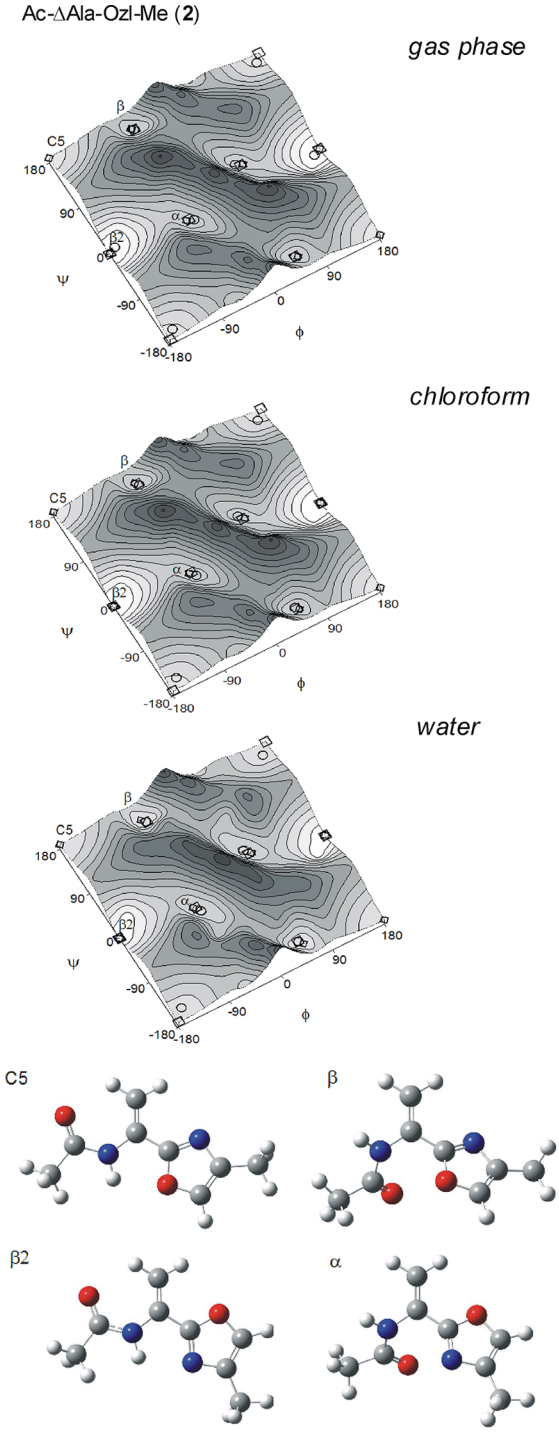

Figure 4. Potential energy surfaces $E = f(\varphi,\psi)$ for Ac-ΔAla-Ozl-Me (**2**) calculated by the M06-2X/6-311++G(d,p) method in gas phase, chloroform, and water. Energy contours are plotted every 1 kcal/mol. Local minima (see Table 1) are calculated at the M06-2X (□), B3LYP (◇), and MP2 (○) levels. The presented conformers were optimized at M06-2X/6-311++G(d,p) in chloroform.

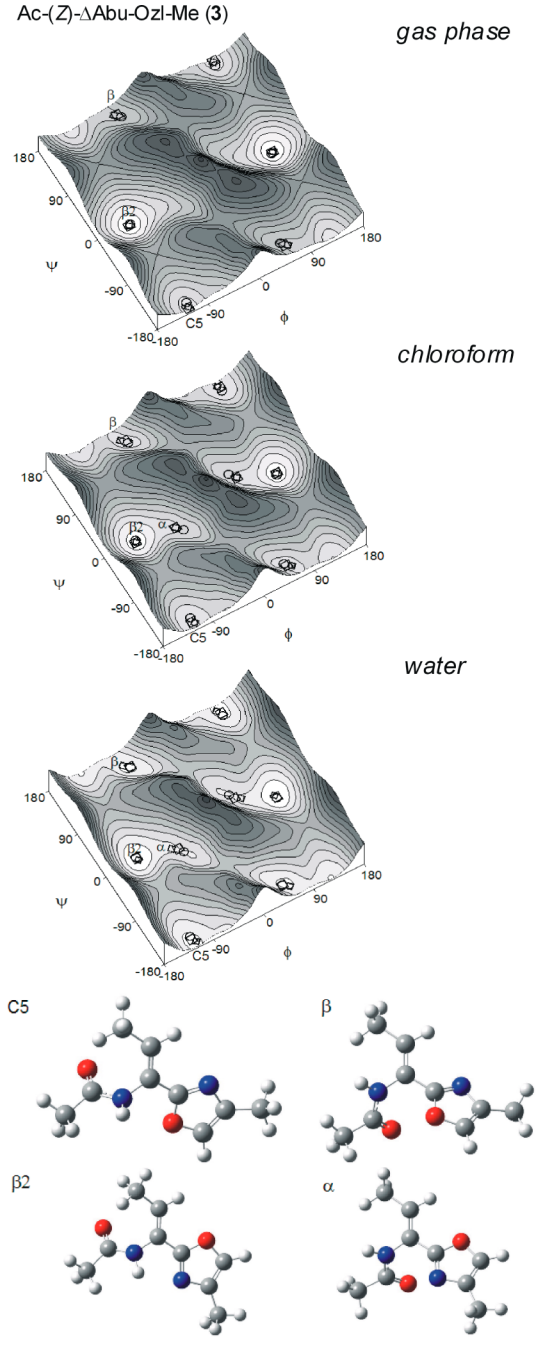

Figure 5. Potential energy surfaces $E = f(\varphi,\psi)$ for Ac-(*Z*)-ΔAbu-Ozl-Me (**3**) calculated by the M06-2X/6-311++G(d,p) method in gas phase, chloroform, and water. Energy contours are plotted every 1 kcal/mol. Local minima (see Table 1) are calculated at the M06-2X (□), B3LYP (◇), and MP2 (○) levels. The presented conformers were optimized at M06-2X/6-311++G(d,p) in chloroform.

determine the conformational properties (Table 2S in the Supporting Information). For all studied compounds, the oxazole hydrogen atom was chosen for irradiation. For Ala-Ozl (**4**) in the $CDCl_3$ solution, irradiation of the signal at δ_H 8.18 gives enhancement of the signal at δ_H 5.01 assigned the hydrogen atom α. This result shows the presence of the conformation $\beta 2$, in agreement with the FTIR and theoretical analyses. In more polar DMSO solution, irradiation of the oxazole hydrogen signal at δ_H 8.81 gives not only enhancement of the signal of the hydrogen atom α at δ_H 4.78 but also the amide one at δ_H 7.60. This suggests a conformational equilibrium, in which the conformations $\beta 2$, β, and α' should be considered. Analysis of the NOE spectra for ΔAla-Ozl (**5**), in both the $CDCl_3$ and DMSO solutions, shows solely proximity of the oxazole hydrogen and the hydrogen β at the position *E* in the side chain. It clearly shows preference toward the conformation $\beta 2$, much stronger than in the case of the

dx.doi.org/10.1021/jp4121673 | J. Phys. Chem. B 2014, 118, 2340−2350

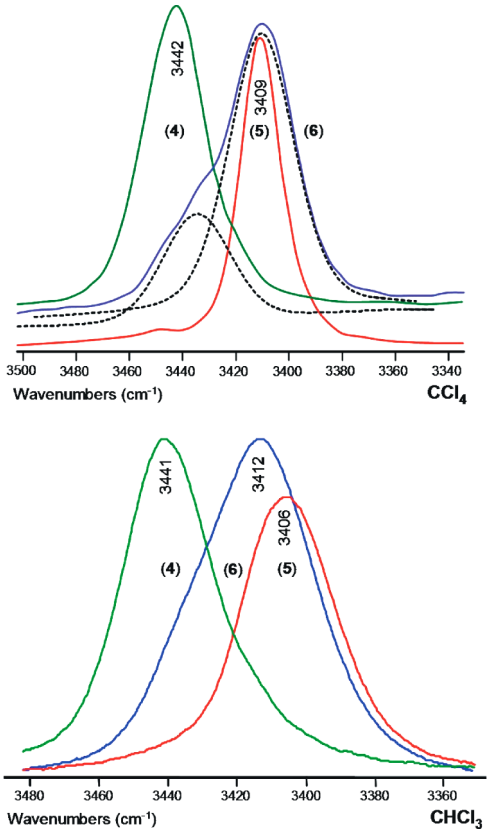

Figure 6. FTIR spectra in CCl_4 and $CHCl_3$, region of the ν_s(N−H), for the molecules **4**−**6**. The component band (dotted line) was obtained by a curve-fitting procedure.

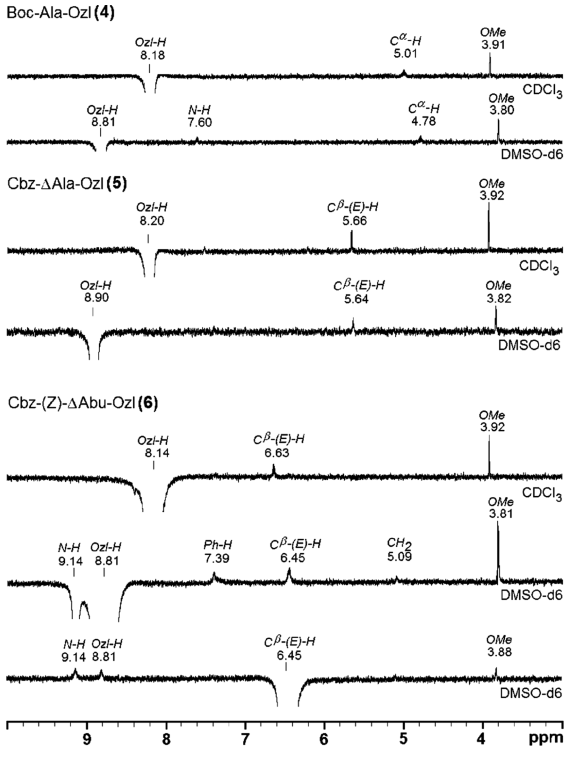

Figure 7. NOE difference spectra in DMSO-d_6 and $CDCl_3$ for **4**−**6**, indicating the correlation between the oxazole hydrogen and the N-terminal amide hydrogen together with the hydrogen α (for **4**) or β at the position E (for **5** and **6**).

saturated alanine analogue **4**. Similar results were obtained for (*Z*)-ΔAbu-Ozl (**6**) in $CDCl_3$ solution. In DMSO solution, because of the proximity of the chemical shifts of the signal for oxazole and amide proton, they both undergo irradiation. However, irradiation of the hydrogen β at δ_H 6.45 gives enhancement of the signal at δ_H 8.81 assigned to the oxazole hydrogen atom. This indicates the presence of the conformation $\beta 2$, although because of enhancement of the signal at δ_H 9.14 assigned to amide hydrogen, other conformations, in particular, β, should be taken into consideration.

Solid-State Crystal Structures. The conformations adopted by compounds **4** and **6** are shown in Figure 8. For

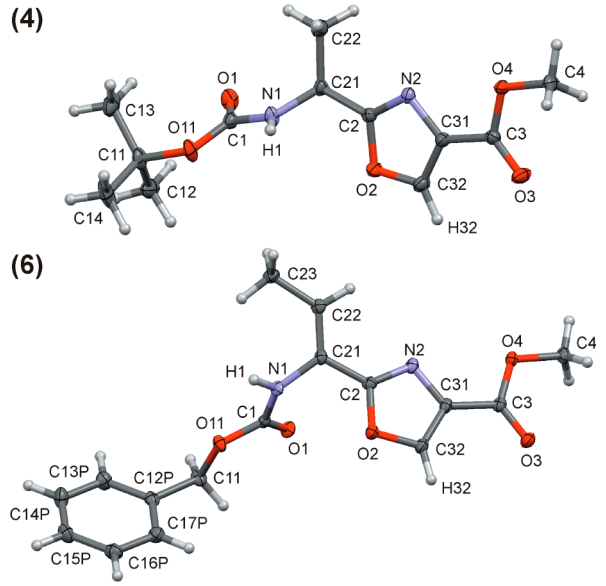

Figure 8. Molecular conformations adopted by **4** and **6** in their solid-state crystal structures. Displacement ellipsoids are plotted at the 50% probability level.

4, the φ and ψ torsion angles are −143.41(17) and −128.9(2)°, respectively. In the case of **6**, the φ and ψ angles equal −62.47(18) and 160.07(14)°. (The opposite φ and ψ angles of 62.47(18) and −160.07(14)°, respectively, were also found for the corresponding symmetry-related molecules presented in the crystal structure.) Figure 9 presents the association pattern of molecules in both studied solids. As can be seen, the intermolecular N−H···O hydrogen bonds are the main interactions, besides the weaker C−H···O hydrogen bonds, responsible for the molecular association (Table 3S in the Supporting Information). A linear arrangement of molecules is observed in both structures. The N-terminal nitrogen atom of each molecule is involved in the N−H···O hydrogen bond being the donor for one molecule, and at the same time the N-terminal oxygen atom serves as a hydrogen-bond acceptor for the other molecule. In **6**, the molecules having the opposite values of the torsion φ and ψ angles form the independent chains.

The comparison with the theoretical results (Table 1) shows that the conformations adopted in the solid state clearly correspond to the calculated conformation α' for **4** and $\beta/-\beta$ for **6**. These conformations are favored in polar environment, which further confirms that intermolecular interactions play an essential role in their stabilization.

dx.doi.org/10.1021/jp4121673 | J. Phys. Chem. B 2014, 118, 2340−2350

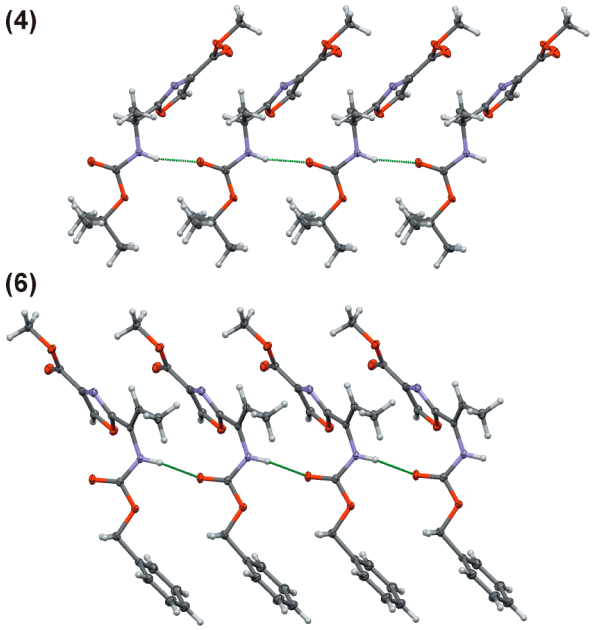

Figure 9. Association patterns of molecules in the crystal structures of **4** and **6**. The dotted green lines indicate the N−H···O hydrogen bonds. Displacement ellipsoids are plotted at the 50% probability level.

Figure 10 presents distribution of the solid-state conformations of oxazole-amino acids[64−75] in various crystal structures retrieved from the Cambridge Structural Database,[76] which are overlaid on the calculated maps. It should be noted that the presented conformations were found for cyclic compounds, which can impose some steric limitations. Also, in the case of the saturated oxazole-amino acids, various side chains, mainly valine, were considered. Nevertheless, the conformations found in the solid state, that is, $\beta 2$, β, α', and αD, clearly correspond to those theoretically calculated. In the case of oxazole-dehydroamino acids, the conformation $\beta 2$ was found for both ΔAla-Ozl and (*Z*)-ΔAbu-Ozl residues.

DISCUSSION

The presented results, both theoretical and spectral, indicate that introduction of the oxazole in the place of C-terminal amide bond causes tendency to adopt the semiextended conformation $\beta 2$. This tendency depends on the environment; it decreases with the increase in polarity environment and it is stronger for the oxazole-dehydroamino acids. In the case of standard alanine model (Ac-Ala-NHMe), the conformation $\beta 2$ can also be found,[47,77] but it has higher energy and is not adopted by the more complex compounds.[78] Previous theoretical studies on dehydroamino acids[48] and esters of dehydroamino acids[46] showed that this conformation could also be adopted but is not energetically favored.

The presented properties of oxazole-amino acids, particularly their tendency toward the conformation $\beta 2$ and lack of tendency toward the conformation C5, can be explained by the electron density distribution around the hetero atoms in the oxazole ring, which differs from the amide group. Oxazole has a little aromatic character,[79] in which both the nitrogen and oxygen atoms are involved. The nitrogen atom shares only one electron with the aromatic sextet with the lone electron pair in the oxazole ring plain. In the case of the amide nitrogen, the lone pair is involved in the amide resonance. This shows that the nitrogen atom in the oxazole should be a stronger hydrogen

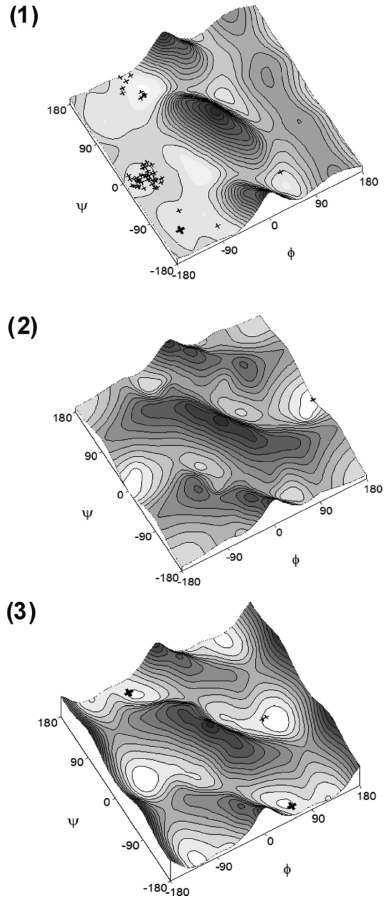

Figure 10. φ, ψ potential energy surfaces of the studied molecules **1**−**3** in a water-mimicking environment together with the solid-state crystal structure conformations of **4** and **6** presented in this work (bold crosses) and analogous structures retrieved from the Cambridge Structural Database (small crosses).

bond acceptor than that in amide. In contrast, the oxygen atom in the oxazole ring shares its electron pair with the aromatic sextet. In the case of amide oxygen, both electron pairs are not involved in the amide resonance. As a consequence, the oxygen in the oxazole ring should be a weaker hydrogen bond acceptor than that in the amide group. The literature reports concerning oxazole indicate that oxygen atom is a weaker hydrogen bond acceptor than nitrogen and forms longer hydrogen bonds.[80] The relatively strong hydrogen bond ability of nitrogen in comparison with oxygen is explained on the basis of its basicity[81] as well as weak nonparticipation in the conjugative interaction of ring cloud.[82] It was shown that proton affinity for the nitrogen atom is substantially higher in comparison with the oxygen atom in the oxazole ring.[83] All of these data support our findings that N−H···N hydrogen bond in the conformation $\beta 2$ is much stronger than N−H···O hydrogen bond in the conformation C5.

The structural differences between the oxazolo-amino acids and oxazolo-dehydroamino acids also influence their conformational stability. The conformations of the oxazolo-dehydroamino acids can be additionally stabilized by possible π-electron conjugation involving oxazole ring and carbon−carbon double bond. This makes the conformation $\beta 2$ more stable than that for saturated oxazolo-amino acids, which was confirmed by the theoretical calculations (Table 1). In the case of the oxazolo-dehydroalanine, the lack of steric hindrance makes the

dx.doi.org/10.1021/jp4121673 | J. Phys. Chem. B 2014, 118, 2340−2350

conformation $\beta 2$ flat, and the π-electron conjugation also involves the N-terminal amide group. Moreover, because of the sp^2 hybridization of the carbon atom α, the donor acceptor distance in the N−H···N hydrogen bond is the shortest in all studied compounds. This is further confirmed by the low position of ν_s(N−H) band (Figure 6) as well as the predominance of the conformation $\beta 2$ even in DMSO environment (Figure 7). In the case of (*Z*)-dehydrobutyrine, the steric hindrance caused by the methyl group in the position *Z* limits the π-electron conjugation to the oxazole ring and double bond, which increases the length of the donor acceptor distance in the intramolecular N−H···N hydrogen bond. Thus, a smaller tendency toward the conformation $\beta 2$ can be predicted. Some additional changes in the electron density within the oxazole ring should be also considered, although their influences are not clear.

CONCLUSIONS

The presented studies show that the stable conformation $\beta 2$ is a characteristic feature of the oxazole-amino acids. The stability of the conformation $\beta 2$ results from the presence of the intramolecular N−H···N hydrogen bond, in which the donor is the N-terminal amide group and the acceptor is the nitrogen atom of the oxazole ring. The strength of the hydrogen bond acceptor results from the aromatic character of oxazole ring. The tendency toward the conformation $\beta 2$ decreases with increasing polarity of the environment, but it also depends on the type of amino acid studied. The conformation $\beta 2$ is more stable for the oxazole-dehydroamino acids, particularly for oxazole-dehydroalanine, in which the lack of steric hindrance in the side chain results in broader π-electron conjugation and shorter N−H···N hydrogen bond. The geometry of the conformation $\beta 2$ is determined by the type of amino acid residue.

The presented studies were based on six selected model compounds of oxazole-amino acids. Therefore, the amount of data can be too small to describe precisely the whole family of compounds. Although the chosen amino acids are found in nature, they contain the simplest side chains. It can be expected that the greater side chain can influence the conformational properties. In particular, phenylalanine and dehydrophenylalanine can be interesting in perspective studies. Nevertheless, the presented results give evaluation of the basic conformational properties of the structural motif, wherein the oxazole ring is placed within amino or dehydroamino acid residue.

ASSOCIATED CONTENT

Supporting Information

Theoretical amide mode frequencies ν_s(N−H) for **1**−**3**. Distances between the selected hydrogen atoms in the conformation of **1**−**3**. Hydrogen-bond geometries in the crystal structures of **4** and **6**. The complete citations for ref 50. This material is available free of charge via the Internet at http://pubs.acs.org.

AUTHOR INFORMATION

Corresponding Author

*Tel: (+48) 77 452 7154. Fax: (+48) 77 452 7101. E-mail: dsiodlak@uni.opole.pl.

Notes

The authors declare no competing financial interest.

ACKNOWLEDGMENTS

This research was partially supported by PL-Grid Infrastructure. We gratefully acknowledge the Academic Computer Centre CYFRONET AGH in Kraków for the calculation facilities and software. M.S. is a recipient of a Ph.D. fellowship from a project funded by the European Social Fund.

REFERENCES

(1) Egawa, Y.; Umino, K.; Tamura, Y.; Shimizu, M.; Kaneko, K.; Sakurazawa, M.; Awataguchi, S.; Okuda, T. Sulfomycins, a Series of New Sulfur-Containing Antibiotics. I. Isolation, Purification and Properties. *J. Antibiot.* **1969**, *22*, 12−17.

(2) Biskupiak, J. E.; Meyers, E.; Gillum, A. M.; Dean, L.; Trejo, W. H.; Kirsch, D. R. Neoberninamycin, a New Antibiotic Produced by *Micrococcus luteus*. *J. Antibiot.* **1988**, *41*, 684−687.

(3) Murakami, T.; Holt, T. G.; Thompson, C. J. Thiostrepton-Induced Gene Expression in *Streptomyces Lividans*. *J. Bacteriol.* **1989**, *171*, 1459−1466.

(4) Lindquist, N.; Fenical, W.; Van Duyne, G. D.; Clardy, J. Isolation and Structure Determination of Diazonamides A and B, Unusual Cytotoxic Metabolites from the Marine Ascidian *Diazona Chinensis*. *J. Am. Chem. Soc.* **1991**, *113*, 2303−2304.

(5) Debono, M.; Molloy, R. M; Occolowitz, J. L.; Paschal, J. W.; Hunt, A. H.; Michel, K. H.; Martin, J. W. The Structure of A10255B, -G, -J: New Thiopeptide Antibiotics Produced by *Streptomyces Gardneri*. *J. Org. Chem.* **1992**, *57*, 5200−5208.

(6) Boeck, L. D.; Berry, D. M.; Mertz, F. P.; Wetzel, R. W. A10255, a Complex of Novel Growth-Promoting Thiopeptide Antibiotics Produced by a Strain of *Streptomyces Gardneri*. Taxonomy and Fermentation Studies. *J. Antibiot.* **1992**, *45*, 1222−1230.

(7) Yun, B.-S.; Hidaka, T.; Furihata, K.; Seto, H. Thiotipin, a Novel Thiopeptide With a TipA Promoter Inducing Activity Produced by *Streptomyces* sp. DT31. *Tetrahedron* **1994**, *50*, 11659−11664.

(8) Lau, R. C. M.; Rinehart, K. L. Biosynthesis of Berninamycin: Incorporation of 13C-Labeled Amino Acids. *J. Am. Chem. Soc.* **1995**, *117*, 7606−7610.

(9) Chiu, M. L.; Folcher, M.; Katoh, T.; Puglia, A. M.; Vohradsky, J.; Bong-Sik, Y.; Haruo, S.; Thompson, C. J. Broad Spectrum Thiopeptide Recognition Specificity of the *Streptomyces lividans* TipAL Protein and Its Role in Regulating Gene Expression. *J. Biol. Chem.* **1999**, *274*, 20578−20586.

(10) Yun, B.-S.; Fujita, K.-I.; Furihata, K.; Seto, H. Absolute stereochemistry and solution conformation of promothiocins. *Tetrahedron* **2001**, *57*, 9683−9687.

(11) Freeman, D. J.; Pattenden, G. Total synthesis and assignment of stereochemistry of raocyclamide cyclopeptides from cyanobacterium Oscillatoria raoi. *Tetrahedron Lett.* **1998**, *39*, 3251−3254.

(12) Nadkarni, S. R.; Mukhopadhyay, T.; Jayvanti, K.; Vijaya Kumar E. K. Eur. Patent 96111156, 1998.

(13) Vijaya Kumar, E. K. S.; Kenia, J.; Mukhopadhyay, T.; Nadkarni, S. R. Methylsulfomycin I, a New Cyclic Peptide Antibiotic from a *Streptomyces* sp. HIL Y-9420704. *J. Nat. Prod.* **1999**, *62*, 1562−1564.

(14) Rodríguez, J. C.; Holgado, G. G.; Sánchez, R. I.; Canedo, L. M. Radamycin, a Novel Thiopeptide Produced by *Streptomyces sp.* RSP9. II. Physico-Chemical Properties and Structure Determination. *J. Antibiot.* **2002**, *55*, 391−395.

(15) Holgado, G. G.; Rodríguez, J. C.; Hernández, L. M. C.; Díaz, M.; Fernández-Abalos, J. M.; Trujillano, I.; Santamaria, R. I. Radamycin, a Novel Thiopeptide Produced by *Streptomyces sp.* RSP9. I. Taxonomy, Fermentation, Isolation and Biological Activities. *J. Antibiot.* **2002**, *55*, 383−399.

(16) Kanoh, K.; Matsuo, Y.; Adachi, K.; Imagawa, H.; Nishizawa, M.; Shizuri, Y. Mechercharmycins A and B, Cytotoxic Substances from Marine-Derived *Thermoactinomyces* sp. YM3−251. *J. Antibiot.* **2005**, *58*, 289−292.

(17) Deeley, J.; Bertram, A.; Pattenden, G. Novel Polyoxazole-Based Cyclopeptides from *Streptomyces* sp. Total Synthesis of the Cyclo-

peptide YM-216391 and Synthetic Studies Towards Telomestatin. *Org. Biomol. Chem.* **2008**, *6*, 1994−2010.
(18) Suzuki, H.; Andoh, M.; Yonezawa, Y.; Akai, S.; Shin, C.; Sato, K. Total Syntheses of Bistratamides J, E, and H from Two Types of δAla-Containing Oligopeptides. *Bull. Chem. Soc. Jpn.* **2008**, *81*, 495−501.
(19) Portmann, C.; Blom, J. F.; Kaiser, M.; Brun, R.; Juttner, F.; Gademann, K. Isolation of Aerucyclamides C and D and Structure Revision of Microcyclamide 7806A: Heterocyclic Ribosomal Peptides from *Microcystis aeruginosa* PCC 7806 and Their Antiparasite Evaluation. *J. Nat. Prod.* **2008**, *71*, 1891−1896.
(20) Raveh, A.; Moshe, S.; Evron, Z.; Flescher, E.; Carmeli, S. Novel Thiazole and Oxazole Containing Cyclic Hexapeptides from a Waterbloom of the Cyanobacterium *Microcystis* sp. *Tetrahedron* **2010**, *66*, 2705−2712.
(21) Chattopadhyay, S. K.; Singha, S. K. Efficient Construction of the Carbon Skeleton of the Novel Polyoxazole-based Cyclopeptide IB-01211 via a Biomimetic Macrocyclisation. *Synlett* **2010**, *4*, 555−558.
(22) Kai, M.; González, I.; Genilloud, O.; Singh, S. B.; Svatos, A. Direct Mass Spectrometric Screening of Antibiotics from Bacterial Surfaces Using Liquid Extraction Surface Analysis. *Rapid. Commum. Mass Spectrom.* **2012**, *26*, 2477−2482.
(23) Bagley, M. C.; Dale, J. W.; Merritt, E. A.; Xiong, X. Thiopeptide Antibiotics. *Chem. Rev.* **2005**, *105*, 685−714.
(24) Jin, Z. Muscarine, Imidazole, Oxazole, and Thiazole Alkaloids. *Nat. Prod. Rep.* **2011**, *28*, 1143−1191.
(25) Dunbar, K. L.; Mitchell, D. A. Insights Into the Mechanism of Peptide Cyclodehydrations Achieved Through the Chemoenzymatic Generation of Amide Derivatives. *J. Am. Chem. Soc.* **2013**, *135*, 8692−8701.
(26) Anderson, I. E.; Batsalova, T.; Dzhambazov, B.; Edvinsson, L.; Holmdahl, R.; Kihlberg, J.; Linusson, A. Oxazole-Modified Glycopeptides That Target Arthritis-Associated Class II MHC A^q and DR4 Proteins. *Org. Biomol. Chem.* **2010**, *8*, 2931−2940.
(27) Ceide, S. C.; Trembleau, L.; Haberhauer, G.; Somogyi, L.; Lu, X.; Bartfai, T.; Rebek, J. Synthesis of Galmic: A Nonpeptide Galanin Receptor Agonist. *Proc. Natl. Acad. Sci. U.S.A.* **2004**, *101*, 16727−16732.
(28) Haberhauer, G.; Pintér, Á.; Oeser, T.; Rominger, F. Synthesis and Structural Investigation of C4- and C 2-Symmetric Molecular Scaffolds Based on Imidazole Peptides. *Eur. J. Org. Chem.* **2007**, *11*, 1779−1792.
(29) Phillips, A. J.; Uto, Y.; Wipf, P.; Reno, M. J.; Williams, D. R. Synthesis of Functionalized Oxazolines and Oxazoles with DAST and Deoxo-Fluor. *Org. Lett.* **2000**, *2*, 1165−1168.
(30) Yeh, V. S. C. Recent Advances in the Total Syntheses of Oxazole-Containing Natural Products. *Tetrahedron* **2004**, *60*, 11995−12042.
(31) Nagaya, A.; Yamagishi, Y.; Yonezawa, Y.; Akai, S.; Shin, C.-G.; Sato, K.-I. Scope and Limitations of a Modified Hantzsch Reaction for the Synthesis of Oxazole-Dehydroamino Acid Derivatives from Dehydroamino Acid Amides. *Heterocycles* **2012**, *85*, 313−331.
(32) Ferreira, P. M. T.; Monteiro, L. S.; Pereira, G. Synthesis of Substituted Oxazoles from N-Acyl-β-hydroxyamino Acid Derivatives. *Eur. J. Org. Chem.* **2008**, *27*, 4676−4683.
(33) Ferreira, P. M. T.; Castanheira, E. M. S.; Monteiro, L. S.; Pereira, G.; Vilaça, H. A Mild High Yielding Synthesis of Oxazole-4-carboxylate Derivatives. *Tetrahedron* **2010**, *66*, 8672−8680.
(34) Lucke, A. J.; Tyndall, J. D. A.; Singh, Y.; Fairlie, D. P. Designing Supramolecular Structures from Models of Cyclic Peptide Scaffolds with Heterocyclic Constraints. *J. Mol. Graph. Mod.* **2003**, *21*, 341−355.
(35) Haberhauer, G.; Drosdow, E.; Oeser, T.; Rominger, F. Structural Investigation of Westiellamide Analogues. *Tetrahedron* **2008**, *64*, 1853−1859.
(36) Rich, H. R.; Bhatnagar, P. K. Conformational Studies of Tentoxin by Nuclear Magnetic Resonance Spectroscopy. Evidence for a New Conformation for a Cyclic Tetrapeptide. *J. Am. Chem. Soc.* **1978**, *100*, 2212−2218.
(37) Imazu, S.; Shimohigashi, Y.; Kodama, H.; Sakaguchi, K.; Waki, M.; Kato, T.; Izumiya, N. Conformationally Stabilized Gramicidin S Analog Containing Dehydrophenylalanine in Place of D-Phenylalanine(4,4′). Synthesis and Antimicrobial Activity. *Int. J. Pept. Protein Res.* **1988**, *32*, 298−306.
(38) Miyashita, M.; Nakamori, T.; Miyagawa, H.; Akamatsu, M.; Ueno, T. Inhibitory Activity of Analogs of AM-Toxin, a Host-Specific Phytotoxin from the *Alternaria alternata* Apple Pathotype, on Photosynthetic O2 Evolution in Apple Leaves. *Biosci. Biotechnol. Biochem.* **2003**, *67*, 635−638.
(39) Latajka, R.; Makowski, M.; Jewgiński, M.; Pawełczak, M.; Koroniak, H.; Kafarski, P. Peptide p-Nitrophenylanilides Containing (*E*)-Dehydrophenylalanine - Synthesis, Structural Studies and Evaluation of Their Activity Towards Cathepsin C. *New J. Chem.* **2006**, *30*, 1009−1018.
(40) Latajka, R.; Jewginski, M.; Makowski, M.; Pawełczak, M.; Huber, T.; Sewald, N.; Kafarski, P. Pentapeptides Containing Two Dehydrophenylalanine Residues - Synthesis, Structural Studies and Evaluation of Their Activity Towards Cathepsin C. *J. Pept. Sci.* **2008**, *14*, 1084−1095.
(41) Ferreira, P. M.; Monteiro, L. S.; Coban, T.; Suzen, S. Comparative Effect of *N*-Substituted Dehydroamino Acids and Alpha-Tocopherol on Rat Liver Lipid Peroxidation Activities. *J. Enzyme Inhib. Med. Chem.* **2009**, *24*, 967−971.
(42) Gupta, M.; Chauhan, V. S. De Novo Design of α,β-Didehydrophenylalanine Containing Peptides: From Models to Applications. *Biopolymers* **2011**, *95*, 161−173.
(43) Siodłak, D.; Gajewska, M.; Macedowska, A.; Rzeszotarska, B. Conformational Studies Into *N*-Methylation of Alanine Diamide Models: A Quantitative Approach. *J. Mol. Struct.: THEOCHEM* **2006**, *775*, 47−59.
(44) Siodłak, D.; Macedowska-Capiga, A.; Broda, M. A.; Kozioł, A. E.; Lis, T. The *Cis-Trans* Isomerization of *N*-Methyl-α,β-Dehydroamino Acids. *Biopolymers* **2012**, *98*, 466−478.
(45) Siodłak, D.; Bujak, M.; Staś, M. Intra- and Intermolecular Forces Dependent Main Chain Conformations of Esters of α,β-dehydroamino acids. *J. Mol. Struct.* **2013**, *1047*, 229−236.
(46) Siodłak, D.; Grondys, J.; Broda, M. A. The Conformational Properties of α,β-Dehydroamino Acids with a C-Terminal Ester Group. *J. Pept. Sci.* **2011**, *17*, 690−699.
(47) Siodłak, D.; Janicki, A. Conformational Properties of the Residues Connected by Ester and Methylated Amide Bonds: Theoretical and Solid State Conformational Studies. *J. Pept. Sci.* **2010**, *16*, 126−135.
(48) Siodłak, D.; Grondys, J.; Lis, T.; Bujak, M.; Broda, M. A.; Rzeszotarska, B. The Conformational Properties of Dehydrobutyrine and Dehydrovaline: Theoretical and Solid-State Conformational Studies. *J. Pept. Sci.* **2010**, *16*, 496−505.
(49) De Marco, R.; Greco, A.; Rupiani, S.; Tolomelli, A.; Tomasini, C.; Pieraccini, S.; Gentilucci, L. In-Peptide Synthesis of Di-Oxazolidinone and Dehydroamino Acid −Oxazolidinone Motifs as β-Turn Inducers. *Org. Biomol. Chem.* **2013**, *11*, 4316−4326.
(50) Frisch, M. J.; Trucks, G. W.; Schlegel, H. B.; Scuseria, G. E.; Robb, M. A.; Cheeseman, J. R.; Scalmani, G.; Barone, V.; Mennucci, B.; Petersson, G. A.; et al. *Gaussian 09*, revision A.02; Gaussian, Inc.: Wallingford, CT, 2009.
(51) Zhao, Y.; Truhlar, D. G. The M06 Suite of Density Functionals For Main Group Thermochemistry, Thermochemical Kinetics, Noncovalent Interactions, Excited States, and Transition Elements: Two New Functionals and Systematic Testing of Four M06 Functionals and 12 Other Functionals. *Theor. Chem. Acc.* **2008**, *120*, 215−241.
(52) *Surfer 8*; Golden Software, Inc.: Golden, CO, 2002.
(53) Schwabe, T.; Grimme, S. Double-Hybrid Density Functionals with Long-Range Dispersion Corrections: Higher Accuracy and Extended Applicability. *Phys. Chem. Chem. Phys.* **2007**, *9*, 3397−3406.
(54) Kang, Y. K.; Byun, B. J.; Park, H. S. Conformational Preference and Cis−Trans Isomerization of 4-Methylproline Residues. *Biopolymers* **2010**, *95*, 51−61.

(55) Miertus, S.; Tomasi, J. Approximate Evaluations of the Electrostatic Free Energy and Internal Energy Changes in Solution Processes. *Chem. Phys.* **1982**, *65*, 239−245.
(56) Tomasi, J.; Mennucci, B.; Cammi, R. Quantum Mechanical Continuum Solvation Models. *Chem. Rev.* **2005**, *105*, 2999−3093.
(57) Buczek, A.; Siodłak, D.; Bujak, M.; Broda, M. A. Effects of Side-Chain Orientation on the Backbone Conformation of the Dehydrophenylalanine Residue. Theoretical and X-ray Study. *J. Phys. Chem. B* **2011**, *115*, 4295−4306.
(58) Martell, A. E.; Herbst, R. M. Condensation of Amides with Carbonyl Compounds: Benzyl Carbamate with Aldehydes and Alpha Keto Acids. *J. Org. Chem.* **1941**, *6*, 878−887.
(59) Yonezawa, Y.; Shin, C.; Ono, Y.; Yoshimura, J.; Dehydrooligopeptides, I. The Facile Coupling of α-Amino Acids with α-Dehydroamino Acids to Dehydrodipeptides. *Bull. Chem. Soc. Jpn.* **1980**, *53*, 2905−2909.
(60) Bilcer, G. M.; Lilly, J. C.; Swanson, L. M.; Comentis, Inc. Patent WO2011/130383 A1, 2011.
(61) *CrysAlis CCD and CrysAlis RED*, version 1.17; Oxford Diffraction Poland: Wroclaw, Poland, 2003.
(62) Sheldrick, G. M. A Short History of *SHELX*. *Acta Crystallogr., Sect. A: Found. Crystallogr.* **2008**, *64*, 112−122.
(63) Macrae, C. F.; Bruno, I. J.; Chisholm, J. A.; Edgington, P. R.; McCabe, P.; Pidcock, E.; Rodriguez-Monge, L.; Taylor, R.; van de Streek, J.; Wood, P. A. *Mercury CSD 2.0* - New Features for the Visualization and Investigation of Crystal Structures. *J. Appl. Crystallogr.* **2008**, *41*, 466−470.
(64) Dong, Y.; Loong, D. T. J.; Yuen, A. K. L.; Black, R. J.; O'Malley, S.; Clegg, J. K.; Lindoy, L. F.; Jolliffe, K. A. Molecular Capsules and Coordination Polymers from a Backbone-Modified Cyclic Peptide Bearing Pyridyl Arms. *Supramol. Chem.* **2012**, *24*, 508−519.
(65) Burgett, A. W. G.; Li, Q.; Wei, Q.; Harran, P. G. A Concise and Flexible Total Synthesis of (−)-Diazonamide A. *Angew. Chem., Int. Ed.* **2003**, *42*, 4961−4966.
(66) Li, J.; Jeong, S.; Esser, L.; Harran, P. G. Total Synthesis of Nominal Diazonamides - Part 1: Convergent Preparation of the Structure Proposed for (-)-Diazonamide A. *Angew. Chem., Int. Ed.* **2001**, *40*, 4765−4770.
(67) Young, P. G.; Clegg, J. K.; Bhadbhade, M.; Jolliffe, K. A. Hybrid Cyclic Peptide-Thiourea Cryptands for Anion Recognition. *Chem. Commun.* **2011**, *47*, 463−465.
(68) Haberhauer, G.; Rominger, F. Syntheses and Structures of Imidazole Analogues of Lissoclinum Cyclopeptides. *Eur. J. Org. Chem.* **2003**, *16*, 3209−3218.
(69) You, S.-L.; Kelly, J. W. The Total Synthesis of Bistratamides F-I. *Tetrahedron* **2005**, *61*, 241−249.
(70) Knowles, R. R.; Carpenter, J.; Blakey, S. B.; Kayano, A.; Mangion, I. K.; Sinz, C. J.; MacMillan, D. W. C. Total Synthesis of Diazonamide A. *Chem. Sci.* **2011**, *2*, 308−311.
(71) Mai, C.-K.; Sammons, M. F.; Sammakia, T. A Concise Formal Synthesis of Diazonamide A by the Stereoselective Construction of the C10 Quaternary Center. *Angew. Chem., Int. Ed.* **2010**, *49*, 2397−2400.
(72) Chen, X.; Esser, L.; Harran, P. G. Stereocontrol in Pinacol Ring-Contraction of Cyclopeptidyl Glycols: The Diazonamide C10 Problem. *Angew. Chem., Int. Ed.* **2000**, *39*, 937−940.
(73) Cheung, C. M.; Goldberg, F. W.; Magnus, P.; Russell, C. J.; Tumbull, R.; Lynch, V. An Expedient Formal Total Synthesis of (-)-Diazonamide A via a Powerful, Stereoselective O Aryl to C-Aryl Migration To Form the C10 Quaternary Center. *J. Am. Chem. Soc.* **2007**, *129*, 12320−12327.
(74) Todorova, A. K.; Jüttner, F.; Linden, A.; Plüss, T.; Von Philipsborn, W. Nostocyclamide: A New Macrocyclic, Thiazole-Containing Allelochemical from *Nostoc* sp. 31 (Cyanobacteria). *J. Org. Chem.* **1995**, *60*, 7891−7895.
(75) Matsuo, Y.; Kanoh, K.; Imagawa, H.; Adachi, K.; Nishizawa, M.; Shizuri, Y. Urukthapelstatin A, a Novel Cytotoxic Substance from Marine-Derived *Mechercharimyces asporophorigenens* YM11−542: II. Physico-Chemical Properties and Structural Elucidation. *J. Antibiot.* **2007**, *60*, 256−260.
(76) Allen, F. H. The Cambridge Structural Database: A Quarter of a Million Crystal Structures and Rising. *Acta Crystallogr., Sect. B* **2002**, *58*, 380−388.
(77) Vargas, R.; Garza, J.; Hay, B. P.; Dixon, D. A. Conformational Study of the Alanine Dipeptide at the MP2 and DFT Levels. *J. Phys. Chem. A* **2002**, *106*, 3213−3218.
(78) Tsai (I-Hsien), M.; Xu, Y.; Dannenberg, J. J. Ramachandran revisited. DFT Energy Surfaces of Diastereomeric Trialanine Peptides in the Gas Phase and Aqueous Solution. *J. Phys. Chem. B* **2009**, *113*, 309−318.
(79) Eicher, T.; Hauptmann, S. *The Chemistry of Heterocycles*; Wiley VCH: Weinheim, Germany, 2003.
(80) Tanzi, L.; Ramondo, F.; Guidoni, L. Vibrational Spectra of Water Solutions of Azoles from QM/MM Calculations: Effects of Solvation. *J. Phys. Chem. A* **2012**, *116*, 10160−10171.
(81) McDonald, N. A.; Jorgensen, W. L. Development of an All-Atom Force Field for Heterocycles. Properties of Liquid Pyrrole, Furan, Diazoles, and Oxazoles. *J. Phys. Chem. B* **1998**, *102*, 8049−8059.
(82) Kaur, D.; Khanna, S. Intermolecular Hydrogen Bonding Interactions of Furan, Isoxazole and Oxazole with Water. *Comput. Theor. Chem.* **2011**, *963*, 71−75.
(83) Kaur, D.; Khanna, S. The Role of Conjugative Interactionsin Acidic and Basic Character of Five Membered Aromatic Heterocyclics. *J.Mol. Struct.: THEOCHEM* **2010**, *949*, 14−22.